Appl Phys A (2011) 104:1047–1051
DOI 10.1007/s00339-011-6358-4

Applied Physics A
Materials Science & Processing

Space-charge relaxation and electrical conduction in $K_{0.5}Na_{0.5}NbO_3$ at high temperatures

Laijun Liu · Yanmin Huang · Congxue Su · Liang Fang · Meixia Wu · Changzheng Hu · Huiqing Fan

Received: 25 November 2010 / Accepted: 23 January 2011 / Published online: 15 March 2011

Abstract Sodium potassium niobate $K_{0.5}Na_{0.5}NbO_3$ (KNN) ceramic was synthesized by a solid-state technique. The X-ray diffraction of the sample at room temperature showed a monoclinic phase. The real part (ε') and imaginary part (ε'') of dielectric permittivity of the sample were measured in a frequency range from 40 Hz to 1 MHz and in a temperature range from 350 to 850 K. The ε' deviated from Curie–Weiss law above 702 K, due to additional dielectric contributions resulting from universal dielectric response and thermally activated space charges at high temperatures. This anomaly arose from a Debye dielectric dispersion that slowed down following an Arrhenius law. We have established a link between the dielectric relaxation and the conductivity.

1 Introduction

High permittivity perovskite materials have numerous technological applications, such as capacitors and memory devices. The permittivity of these materials generally varies hugely with temperature, a property which is unfavorable for many applications due to bad temperature stability. Recently, lead-free piezoelectric ceramics have received increasing attention from the viewpoint of environmental protection on the earth. Sodium potassium niobate, $K_{1-x}Na_xNbO_3$-based ceramics are one of the most promising alternative systems to lead-based ceramics [1, 2]. Compounds in $K_{1-x}Na_xNbO_3$ system are isostructural with $KNbO_3$ and $NaNbO_3$ [3]. The compound $K_{0.5}Na_{0.5}NbO_3$ (KNN) lies near a morphotropic phase boundary between two orthorhombic phases in the $KNbO_3$–$NaNbO_3$ pseudobinary system [4, 5]. KNN has an orthorhombic–tetragonal transition at ∼200°C and a tetragonal–cubic transition at ∼400°C [6].

The dielectric properties of KNN-based ceramics at high temperatures are rarely studied due to the large dielectric loss, and few high temperature applications. However, the benefit of high temperature dielectric investigation is the ability to distinguish a material's space charge and defects/carriers contributions which are resolved in impedance measurements [7–9]. Furthermore, these contributions can vary significantly with preparation conditions, chemical modifications as well as the measurement of temperature range [10–15]. An ideal ferroelectric, such as $Na_{0.5}K_{0.5}NbO_3$ (KNN) should be a good electrical insulator, and its dielectric permittivity follows Curie–Weiss law above Curie temperature. However, there is a more complex reason for the decrease in insulating properties. Various relaxation processes seem to coexist in real KNN ceramics, which contain number of different energy barriers due to point defects (cation and oxygen vacancies) appearing during technological process. The value of relaxation frequency may range from low to high frequencies depending on the type of chemical or physical defects related to the dipoles considered. As a result, defects may cause modifications of the short and/or long-range interactions in inorganic ferroelectrics [16]. An analysis of these contributions

L. Liu (✉) · Y. Huang · C. Su · L. Fang · M. Wu · C. Hu
State Key Laboratory Breeding Base of Nonferrous Metals and Specific Materials Processing, Key laboratory of New Processing Technology for Nonferrous Metal and Materials, Ministry of Education, College of Material Science and Engineering, Guilin University of Technology, Guilin, 541004, China
e-mail: ljliu2@163.com
Fax: +86-773-5893395

H. Fan
State Key Laboratory of Solidification Processing, School of Materials Science and Engineering, Northwestern Polytechnical University, Xi'an 710072, China

provides valuable information that allows effects to be separated [17, 18].

In the present work, we have carried out extensive and systematic studies on dielectric properties of KNN synthesized by a solid-state technique. An analysis of the dielectric and conductivity both as a function of temperature and frequency were carried out on KNN ceramics using an impedance analyzer. The respective data were analyzed by the augmented Jonscher relation and the Arrhenius law. The results are discussed in light of inadvertent contributions of universal dielectric response and thermally activated space charges to high temperature dielectric response in KNN ceramics.

2 Materials and methods

Carbonates and oxides Na_2CO_3, $K_2CO_3{\cdot}1.5H_2O$ and Nb_2O_5 were used as starting materials. Perovskite NKN powder was obtained by milling 450 rpm for 2 h and then calcined at 850°C for 2.5 h. The calcined powder was pressed into discs uniaxially of 10 mm in diameter and 2 mm in thickness under 300 MPa and then pressed under 650 MPa with a cool isostatic pressing method. The discs were sintered at 1090°C for 4 h in an alumina crucible.

X-ray diffraction patterns were obtained using an automated diffractometer (XRD; SIEMENS D5000) with Cu $K_{\alpha 1}$ radiation. Both sides of the samples were sputtered gold electrodes. Electrical properties measurement was taken with an applied voltage of 500 mV over the frequency range 40 Hz to 5 MHz from 350 K to 850 K with an impedance analyzer (Agilent 4294A).

3 Results and discussion

Figure 1 shows the x-ray-diffraction pattern of the sample taken at room temperature. All the reflection peaks of the x-ray profiles were indexed, and lattice parameters were determined using the least-squares method with the help of FullProf software. A good agreement between the observed and calculated interplaner spacings (d values) suggests that the compound is having a monoclinic structure and Pm space group (SG no 6) at room temperature with $\beta = 90.3302$, $a = 4.0032$ Å, $b = 3.9452$ Å, and $c = 4.0032$ Å.

For a normal ferroelectric, such as pure $BaTiO_3$, the Curie–Weiss law is satisfied above the Curie temperature, T_C:

$$\frac{1}{\varepsilon'} = \frac{(T - T_{CW})}{C} \tag{1}$$

where T_{CW} is the Curie–Weiss temperature, and C is the Curie constant. The reciprocal of dielectric permittivity at

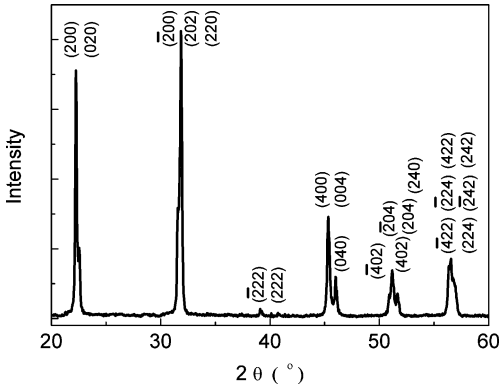

Fig. 1 X-ray powder diffraction pattern obtained at room temperature for KNN and indexed with monoclinic indices

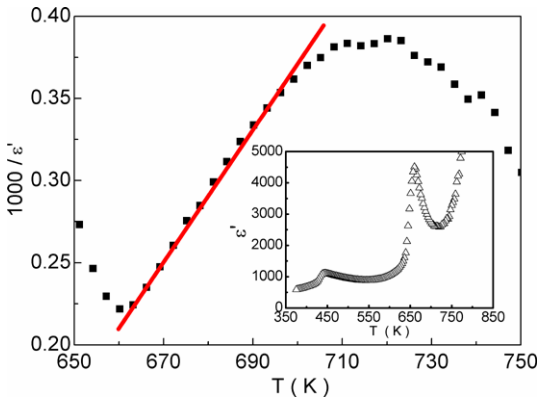

Fig. 2 Temperature dependence of $1000/\varepsilon'$ of KNN ceramics at 1 kHz. The *solid straight line* is the best fit according to (1); Temperature dependence of the dielectric permittivity of KNN at 1 kHz (*inset*)

1 kHz as a function of temperature for the KNN ceramics is shown in Fig. 2. Inset shows the temperature dependence of the dielectric permittivity of KNN at 1 kHz. Here, the T_C of KNN is observed to be 660 K. It can be seen that the dielectric permittivity follows the Curie–Weiss law well at temperatures near T_C. A deviation occurs at higher temperatures ($T > 702$ K), due to additional dielectric contribution resulting possibly from universal dielectric response and thermally activated space charges at high temperatures.

In many relaxor ferroelectrics [19], such as $BaZr_{1-x}Ti_xO_3$ [20, 21], $BaSn_{1-x}Ti_xO_3$ [22, 23] and $PbMg_{1/3}Nb_{2/3}O_3$ [24, 25], the dielectric dispersion slope of permittivity maximum at the high temperatures ($T > T_m$) is very weak in comparison with the relaxation at $T < T_m$. Bokov and Ye [26–29] first found that the dielectric dispersion in $PbMg_{1/3}Nb_{2/3}O_3$-$PbTiO_3$ (PMN-PT) exactly follows the universal dielectric response law at the temperatures above T_m. Figure 3 shows the frequency dependence of the real and imaginary part of the dielectric permittivity of KNN above T_C($T_m = T_C$ for normal ferroelectric KNN). The $\varepsilon'(f)$ significantly decreases with increasing frequency

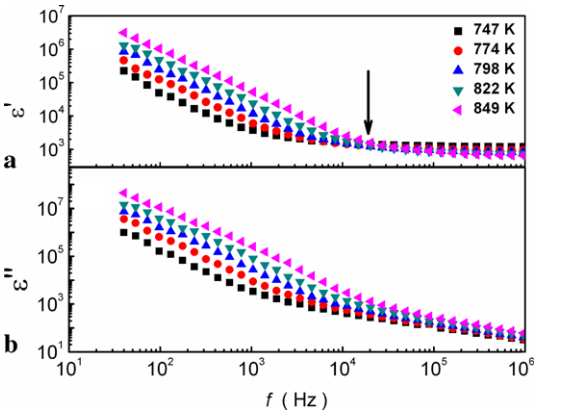

Fig. 3 Frequency dependences of the real part ε' (**a**) and imaginary part ε'' (**b**) of dielectric permittivity of KNN at various temperatures

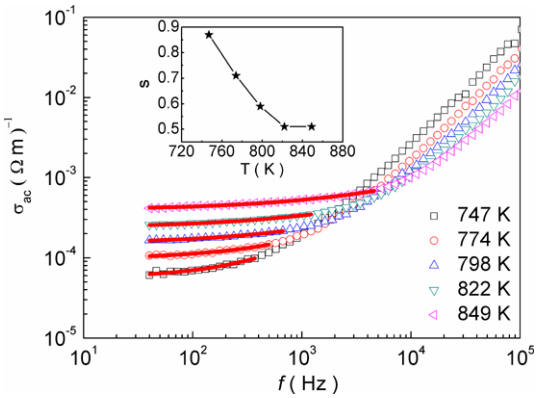

Fig. 4 Frequency dependence of the real part of ac conductivity of KNN. The solid lines are the fit according to (3). The *inset* shows the evolution of the exponent s

while it increases apparently with the increase in temperature below ~10 kHz. In contrast, the dielectric permittivity of KNN weakens with the increase in temperature at high frequency. It can be considered that dielectric diffuses at low frequency and high frequency arise from thermally activated space charges and thermally assisted tunneling process, respectively. As can be seen in Fig. 3b, the $\varepsilon''(f)$ related to the relaxation process also decreases monotonically with increasing frequency at low frequencies (guided by solid lines), which is more clearly shown in the ac conductivity plots.

The frequency-dependent conductivity is given by

$$\sigma' = \varepsilon_0 \varepsilon' \omega \tan\delta \tag{2}$$

Here, σ' is the real part of ac conductivity. Figure 4 displays the frequency dependence of the real part of ac conductivity of KNN at various temperatures. The conductivity shows a dispersion which shifts to the higher-frequency side with the increase of temperature. It is seen from Fig. 4 that σ' decreases with decreasing frequency and becomes independent

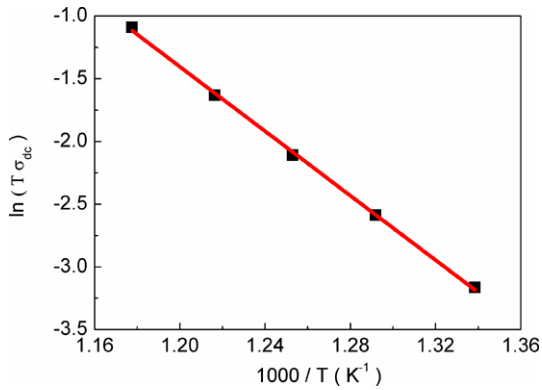

Fig. 5 Arrhenius plot of the dc conductivity of KNN. The squares are the experimental points and the solid line is the least-squares straight–line fit

of frequency after a certain value. Extrapolation of this part toward lower frequency will obtain direct current conductivity (σ_{dc}). Obviously, it could be described by the so-called "universal dielectric response" law

$$\sigma'(f) = \sigma_{dc} + \sigma_0 f^s \tag{3}$$

where σ_{dc} is the dc bulk conductivity and f is the frequency. Equation (3) is typical of thermally assisted tunneling between localized states. This law describes one phenomenon that is associated with many-body interactions between charges and dipoles. By using (3), we get the exponent s as shown in the inset of Fig. 4. It can be found that s decreases rapidly with increasing temperature below 822 K, above which it gets to a plateau value. This result agrees well with Fig. 3a, i.e., the thermally assisted tunneling will weaken at high temperature. Moreover, it is suggested that the value of dielectric permittivity contributed by the universal relaxation process is much less than the thermally activated space charges at high temperatures.

The temperature variation of σ_{dc} thus obtained follows the Arrhenius law given by

$$\sigma_{dc} = T^{-1}\sigma_0 \exp\left(-\frac{E_{con}}{k_B T}\right) \tag{4}$$

with activation energy $E_{con} = 1.11$ eV, as shown in Fig. 5.

Figure 6 shows a complex-plane impedance plot, $Z*$ plot of KNN, plotting the imaginary part Z'' against the real part Z'. Only one arc for each temperature and a approaching zero intercept in horizontal (inset) are presented. Stumpe et al. [30] reported that dielectric relaxation occurred in the temperature range 600–950 K for $SrTiO_3$ and 700–1100 K for $BaTiO_3$. They considered these relaxations as the combined effect of bulk and surface properties, namely, Maxwell–Wagner polarization. The Maxwell–Wagner effect or interfacial phenomena model [31] was usually adopted to explain the dielectric relaxation with extremely high permittivity. Such material consisted of grains separated by

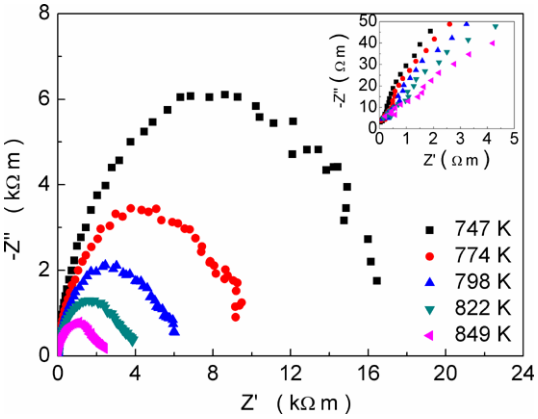

Fig. 6 Complex-plane impedance plots for KNN at different temperatures. The *inset* shows an expanded view of the high-frequency data near the origin

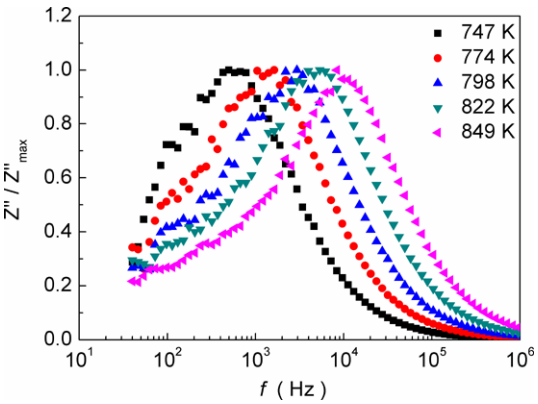

Fig. 7 Normalized imaginary parts, $Z''/Z''_{\max}$ of impedance as a function of frequency

more insulating inter grain barriers. Therefore, for a bulk crystal containing interfacial boundary layers, the equivalent circuit may be considered as two parallel RC elements connected in serial and giving rise to two arcs in complex plane: one for the bulk crystal (grain) and the other for the interfacial boundary (grain-boundary) response. However, the electrically heterogeneous in KNN have not been found since the impedance data show only a large arc with a ~zero high frequency intercept. It is suggested that the high temperature dielectric relaxation does not arise from heterogeneous medium effect (described under the Maxwell–Wagner model).

Maglione et al. [32] reported dielectric relaxation phenomena in many perovskite materials, such as in $CaTiO_3$-, $BaTiO_3$-, and $PbTiO_3$-based systems. They found that the dielectric relaxation was closely related to the oxygen vacancies in these samples. The activation energy for dielectric relaxation is around 1.17–1.48 eV, and the activation energy of conduction is in the range of 1.07–1.31 eV, for $PbTiO_3$ doped with La. The activation energy for conduction of KNN is consistent with this range.

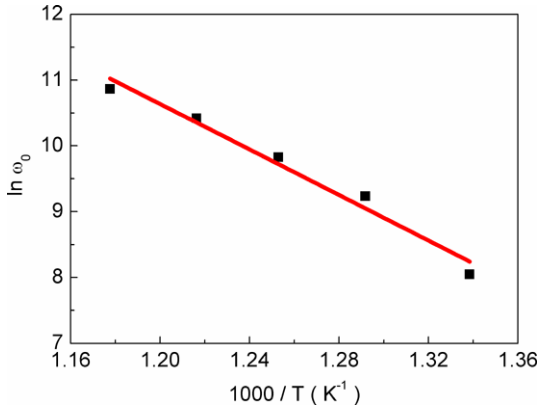

Fig. 8 Temperature dependence of the most probable relaxation frequency obtained from the normalized imaginary part of impedance plots for KNN. The *squares* are the experimental points and the *solid line* is the least-squares straight-line fit

The normalized imaginary parts $Z''/Z''_{\max}$ of impedance as a function of frequency in KNN at several temperatures was shown in Fig. 7. It seems from the figure that at high temperature triggers a relaxation process. The $Z''/Z''_{\max}$ parameter exhibits a peak with a slightly asymmetric degree at each temperature especially at higher temperatures. At the peak, the relaxation is defined by the condition

$$\omega_{\max}\tau_{\max} = 1 \tag{5}$$

where $\tau_{\max}$ is relaxation time. The relaxation frequency in Fig. 8 obeys the Arrhenius relation given by

$$\omega_{\max} = \omega_0 \exp\left[-\frac{E_{\mathrm{rel}}}{k_{\mathrm{B}}T}\right] \tag{6}$$

where ω_0 is preexponential factor. The activation energy E_{rel} calculated from the $\ln \omega_{\max} - 1000/T$ data. The calculated activation energy and preexponential factor of KNN are 1.49 eV and 4.29×10^{13} Hz, respectively.

It is observed that the activation energy for relaxation frequency of charge carriers is more than that for the activation energy for conduction. It is known that the activation energy for conduction (E_{con}) is the sum of both the creation of charge carriers and migration or hopping free energy of charge carriers over a long distance while the activation energy for relaxation frequency of charge carriers (E_{rel}) is equal to the migration free energy of charge carriers and hopping of these charge carriers between the adjacent lattice sites [33]. The activation energy for relaxation and the activation energy of conduction are consistent with those activation energies of oxygen vacancies in perovskite. Similarly to modified lead zirconate titanate ceramics, the KNN ceramics are considered as materials with p-type conductivity due to the high volatility of the sodium/potassium oxide during the applied heat treatments at high temperatures [34]. This

phenomenon provides sodium/potassium and oxygen vacancies. It is known that cation vacancies are quenched defects at low temperatures and such vacancies could become mobile at higher temperatures, with high activation energy values (>2 eV) [35]. Oxygen vacancies have reported activation energies in the range 0.3–0.5 eV for single-ionized oxygen vacancies and 0.6–1.2 eV for doubly-ionized oxygen vacancies, respectively [36–41].

As a consequent, there is a probability of formations of double ionized oxygen vacancy with the release single/two electrons due to heating the samples at elevated temperatures according to the Kroger–Vink notation as given below [42].

$$V_O' = V_O'' + e' \quad \text{or} \quad V_O = V_O'' + 2e' \tag{7}$$

where V_O is the loss of lattice oxygen, V_O' or V_O'' is the presence of oxygen-ion vacancy and e' is the electron released or captured.

Oxygen vacancies facilitate the appearance of dipoles formed with an adjacent host ion and enlarge the rattling space available for dipole vibration, which as a consequence leads to the short-range hopping of the ions and gives rise to relaxation. Besides, the oxygen ion jumps, between the vacancies, are considered to be responsible for the transition from short-range to long-range hopping and may explain the marked ionic conductivity.

4 Conclusions

We have evidenced a diffuse dielectric anomaly in KNN above Curie temperature. The high-temperature dielectric anomaly resulting from thermally activated space charges and thermally assisted tunneling process was investigated. This anomaly arose from a monodispersive Debye-type dielectric relaxation. The value of dielectric permittivity contributed by the universal relaxation process is much less than the thermally activated space charges at high temperatures. Increasing the temperature resulted in an acceleration of the space-charge relaxation, which leaded to an increase of both the conductivity and the dielectric relaxation amplitude. Moreover, the relaxation rate followed the same thermally activated law as the dc conductivity.

Acknowledgements This work was financially supported by Natural Science Foundation of China (Grant Nos. 51002036 and 50962004), and by Natural Science Foundation of Guangxi (Grant Nos. C013002, 0832003Z, and 0832001).

References

1. Y. Saito, H. Takao, T. Tani, T. Nonoyama, K. Takatori, T. Homma, T. Nagaya, M. Nakamura, Nature **432**, 84–87 (2004)
2. E. Hollenstein, M. Davis, D. Damjanovic, N. Setter, Appl. Phys. Lett. **87**, 1–3 (2005)
3. G. Shirane, R. Newnham, R. Pepinsky, Phys. Rev. **96**, 581–588 (1954)
4. B. Jaffe, W.R. Cook Jr., H. Jaffe, *Piezoelectric Ceramics* (Academic Press, London, 1971)
5. M. Ahtee, A.M. Glazer, Acta Crystallogr. **A32**, 434–446 (1976)
6. V.J. Tennery, K.W. Hang, J. Appl. Phys. **39**, 4749–4753 (1968)
7. E. Atamanik, V. Thangadurai, Mater. Res. Bull. **44**, 931–936 (2009)
8. S. Lanfredi, L. Dessemond, A. Rodrigues, J. Am. Ceram. Soc. **86**, 291–298 (2003)
9. Y. Zhen, J. Li, J. Am. Ceram. Soc. **89**, 3669–3675 (2006)
10. T. Takenaka, H. Haneda, K. Kato, M. Takata, K. Shinozaki, Key Eng. Mater. **421–422**, 9–12 (2009)
11. L. Liu, H. Fan, L. Fang, X. Chen, H. Dammak, M. Pham Thi, Mater. Chem. Phys. **117**, 138–141 (2009)
12. E. Atamanik, V. Thangadurai, J. Phys. Chem. C **113**, 4648–4653 (2009)
13. Y.J. Wu, Y.Q. Lin, S.P. Gu, X.M. Chen, Appl. Phys. A, Mater. Sci. Process. **97**, 191–194 (2009)
14. M.A.L. Nobre, S. Lanfredi, J. Phys., Condens. Matter **12**, 7833 (2000)
15. J.L. Dellis, I.P. Raevsky, S.I. Raevskaya, L.A. Reznitchenko, Ferroelectrics **318**, 169–177 (2005)
16. C. Elissalde, J. Ravez, J. Mater. Chem. **11**, 1957–1967 (2001)
17. E. Buixaderas, V. Bovtun, M. Kempa, M. Savinov, D. Nuzhnyy, F. Kadlec, P. Vaněk, J. Petzelt, M. Eriksson, Z. Shen, J. Appl. Phys. **107**, 014111 (2010)
18. V. Bobnar, J. Holc, M. Hrovat, M. Kosec, J. Appl. Phys. **101**, 074103 (2007)
19. Z.G. Ye, Key Eng. Mater. **155–156**, 81 (1998)
20. Z. Yu, C. Ang, R. Guo, A.S. Bhalla, J. Appl. Phys. **92**, 2655 (2002)
21. S. Ke, H. Fan, H. Huang, H.L.W. Chan, S. Yu, J. Appl. Phys. **104**, 034108 (2008)
22. X.Y. Wei, Y.J. Feng, X. Yao, Appl. Phys. Lett. **83**, 2031 (2003)
23. C. Lei, A. Bokov, Z.G. Ye, Ferroelectrics **339**, 129–136 (2006)
24. A.A. Bokov, Z.G. Ye, J. Phys., Condens. Matter **12**, L541 (2000)
25. A.A. Bokov, Z.G. Ye, Phys. Rev. B **65**, 144112 (2002)
26. A.A. Bokov, Z.G. Ye, Phys. Rev. B **74**, 132102 (2006)
27. A.A. Bokov, Z.G. Ye, Phys. Rev. B **66**, 064103 (2002)
28. A.A. Bokov, Z.G. Ye, Solid State Commun. **116**, 105 (2000)
29. A.A. Bokov, Y.H. Bing, W. Chen, Z.G. Ye, S.A. Bogatina, I.P. Raevski, S.I. Raevskaya, E.V. Sahkar, Phys. Rev. B **68**, 052102 (2003)
30. R. Stumpe, D. Wagner, D. Bauerle, Phys. Status Solidi A **75**, 143 (1983)
31. A.R. von Hippel, *Dielectrics and Waves* (Wiley, New York, 1954)
32. O. Bidault, P. Goux, M. Kchikech, M. Belkaoumi, M. Maglione, Phys. Rev. B **49**, 7868 (1994)
33. A. Molak, E. Ksepko, I. Gruszka, A. Ratuszna, M. Paluch, Z. Ujma, Solid State Ion. **176**, 1439–1447 (2005)
34. Y. Xu, *Ferroelectric Materials and Their Applications* (Elsevier Science, Amsterdam, 1991)
35. B. Guiffard, E. Boucher, L. Eyraud, L. Lebrun, D. Guyomar, J. Eur. Ceram. Soc. **25**, 2487 (2005)
36. C. Verdier, F.D. Morrison, D.C. Lupascu, J.F. Scott, J. Appl. Phys. **97**, 024107 (2005)
37. H.I. Yoo, C.R. Song, D.K. Lee, J. Electroceram. **8**, 5 (2002)
38. D.M. Smyth, J. Electroceram. **11**, 89 (2003)
39. R. Moos, W. Menesklou, K.H. Härdtl, Appl. Phys. A **61**, 389 (1995)
40. R. Moos, K.H. Härdtl, J. Appl. Phys. **80**, 393 (1996)
41. M. Maglione, M. Belkaoumi, Phys. Rev. B **45**, 202 (1992)
42. F.A. Kroger, H. Vink, J. Solid State Phys. **3**, 307 (1956)